

HORIZONTALLY ALIGNED CARBON NANOTUBE SCAFFOLDS FOR FREESTANDING STRUCTURES WITH ENHANCED CONDUCTIVITY

Cinzia Silvestri^{*1}, Federico Marciano¹, Bruno Morana^{1, 2}, Violeta Podranovic¹, Sten Vollebregt¹, Guo Qi Zhang¹, Pasqualina M. Sarro¹

¹Delft University of Technology, ECTM-EKL, Delft, THE NETHERLANDS

² Institute of Materials for Electronics and Magnetism, Trento-FBK Division, Trento, ITALY

ABSTRACT

An unprecedented enhancement in electrical conductivity of horizontally aligned carbon nanotube (HA-CNT) structures using a 10 nm conformal coating of alumina (Al_2O_3) or amorphous silicon carbide (a-SiC) is presented. By combining the capability to grow long vertically aligned CNTs (VA-CNTs) with a liquid-assisted flattening technique, dense arrays of HA-CNTs exhibiting a high degree of alignment are realized and integrated at wafer-scale. Suspended structures, ranging from large area membranes to narrow beams, can be fabricated. The impressive enhancement in electrical conductivity, approximately 209% for the Al_2O_3 coated HA-CNTs ($\text{Al}_2\text{O}_3/\text{HA-CNTs}$) and 2276% for the a-SiC ones (a-SiC/HA-CNTs), demonstrates the potential of CNT-based scaffolds as scalable and functional building blocks for suspended interconnects, heat spreaders and novel chemical and optical sensors.

INTRODUCTION

Since their discovered, CNTs have been extensively studied for their outstanding electrical, thermal, optical and mechanical properties. Unfortunately, these excellent properties are difficult to be preserved in macroscopic applications [1]. A typical and versatile CNT construct consists of VA-CNTs. The fast growth rate, the high packing density and the possibility to synthesize CNTs in lithographically defined locations, make them really attractive for various applications such as interconnects [2], on-chip cooling [3], microelectrode arrays [4] and solid-state super capacitors [5], in which the high-aspect ratio and the large surface area are crucial features.

However, for applications like chemical and optical sensing and heat spreading, a VA-CNT structure can be unpractical. Therefore, HA-CNT sheets are needed. This planar arrangement shows higher robustness than the VA counterpart, thus increasing the possibility to introduce CNTs in standard microfabrication processes. To obtain HA-CNTs at wafer scale, two options are available: in-situ synthesis of horizontally aligned CNTs [6-7], or permutation from VA-CNT to HA-CNT induced by external stimulations. The first approach is limited in its applicability by the catalyst deposition techniques to promote the tubes growth, thus obtaining low CNT density. To integrate massive quantity of HA-CNTs into MEMS/NEMS devices, the self-assembly and the horizontal redirection of VA-CNTs by external stimulation is the most suitable solution. The permutation can be mechanically induced [8], liquid induced by immersion or evaporation [9-10], or layer-by-layer assembly given by a combination of manual handling and bonding through liquid densification [11]. Most of the

above mentioned techniques require custom made systems or involve heavy manual handling. In this work, the liquid-assisted flattening technique reported in [9] is used, because it does not require a sophisticated system and it is suitable for wafer-scale processing.

Recently, it has been demonstrated that by infiltrating nanoscale conformal coatings on CNT nanofoams is possible to tune their mechanical behavior [12]. This procedure is a valuable alternative to effectively enhance the material properties of nanofoam like materials.

Here we present a method to use the foam-like morphology of the CNT array as scaffold for creating reinforced heterostructures with tailored material properties, among others the electrical conductivity. After the synthesis of VA-CNT on a pre-processed wafer, the liquid-assisted flattening is performed. The obtained HA-CNT sheets are subjected to a nanometer scale conformal coatings of Al_2O_3 or a non-stoichiometric a-SiC, both with a targeted thickness of 10 nm. By characterizing the electrical properties of the HA-CNTs prior and after the coating infiltration, the performance increase in terms of effective electrical conductivity of CNTs is extracted.

FABRICATION/EXPERIMENTAL

Pre-patterned wafer

HA-CNT structures, such as suspended interconnects and membranes, are formed directly on predefined areas of a 4" silicon (Si) wafer. A schematic drawing, illustrating the cross-sectional view of the two structures, is depicted in figure 1a.

The silicon oxide (SiO_2) pillars of the suspended interconnect vary in shape, spacing and number. Their height can be determined through the deep reactive ion etching (DRIE) process ranging from 1 μm to 7 μm . The membrane is made by 200 nm low-pressure chemical vapor deposition (LPCVD) silicon nitride (SiN). The contact electrodes for both structures are made of a layer stack of 20 nm of tantalum (Ta) and 160 nm of platinum (Pt). The distance among the electrodes is varied depending on the targeted height of the CNTs.

CNT growth

The CNTs are synthesized on a 30 nm thin barrier layer of sputtered Al_2O_3 on which a 1.8 nm evaporated iron (Fe) catalyst is patterned by lift-off to define rectangles of 10 μm in thickness (T) and a width (W) ranging from 30 μm to 800 μm , depending on the envisioned application (Figure 1.b and c). The wafer is then loaded in a commercial chemical vapor deposition (CVD) system (Axiotron, Black Magic) at 650°C for 5 minutes using $\text{H}_2/\text{C}_2\text{H}_2$ as feedstock at a pressure of 80 mbar.

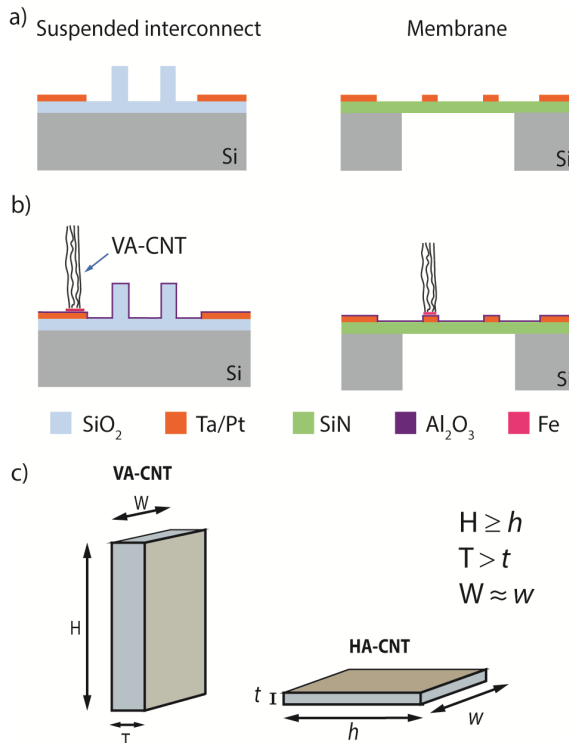


Figure 1: Key process steps for the fabrication of HACNT sheets. Schematic cross-section (not to scale) of the two structures considered in the current study, (a) before and (b) after the VA-CNT synthesis. (c) A well oriented HACNT is achieved by defining the aspect ratio between the width (W) and thickness (T) of the catalyst island to be more than 10 for $T \leq 10\mu\text{m}$ and more than 5 for $T > 10\mu\text{m}$. The obtained HACNT sheet retains the original width and has a slightly increased height, while the thickness strongly decreases due to the CNT densification.

Flattening procedure

The liquid-assisted flattening process consists in inducing the VA-CNT densification and the horizontal alignment by capillary adhesion through the immersion in isopropyl alcohol (IPA) and the withdrawal of the sample. To achieve the desired HACNT sheets, the wafer was perpendicularly immersed in the solution and then dried at ambient temperature while kept at a tilting angle of 45° (Fig. 2). After removing the sample from the solution, a thin layer of IPA infiltrates the VA-CNT nanofoam and wets the substrates forming a meniscus around the microstructure sidewall. The VA-CNT experiences shrinkage towards the structure barycenter due to the internal capillary forces and the strong Van der Waals interactions. The resulting structure is smaller and unbalanced, due to the densification, and tends to fold into a given direction. Then, the IPA layer trapped between the CNT sidewall and the substrate produces attractive forces, thus pushing the CNT array downward onto the substrate and forming the HACNT sheet.

Coating Procedure

The obtained HACNT structures (Fig. 2) were coated with a 10 nm thin film of a-SiC or Al₂O₃ by LPCVD or atomic layer deposition (ALD), respectively. The a-SiC layer is obtained using acetylene (C₂H₂) and dichlorosilane (SiH₂Cl₂) diluted in 5% hydrogen (H₂)

and the deposition temperature and pressure are fixed at 760°C and 0.8 mbar, respectively. The a-SiC deposition rate is ~5 Å min⁻¹. The Al₂O₃ ALD layer is performed on an ASM F-120 reactor at a set temperature and pressure of 300°C and 1.33 mbar, respectively. The precursor gases are Trimethylaluminum (TMA) and deionized water (H₂O). The average Al₂O₃ deposition rate is self-limited to ~0.9 nm cycle⁻¹. At this stage two hybrid composite based on CNT scaffolds are obtained, namely Al₂O₃/HA-CNTs and a-SiC/HA-CNTs.

Characterization

The morphology, the packing density and the quality of CNTs were monitored after performing the crucial fabrication steps: VA-CNT growth, permutation in HA-CNTs and after the coating infiltrations. This information was collected by acquiring the CNT Raman spectra, through a Renishaw's inVia Raman microscope with 514 nm laser wavelength, and by scanning electron microscopy (SEM, Philips XL50) inspection. The I-V characteristics were performed on a Cascade probe station and an Agilent 4156C Semiconductor Parameter Analyzer in DC mode.

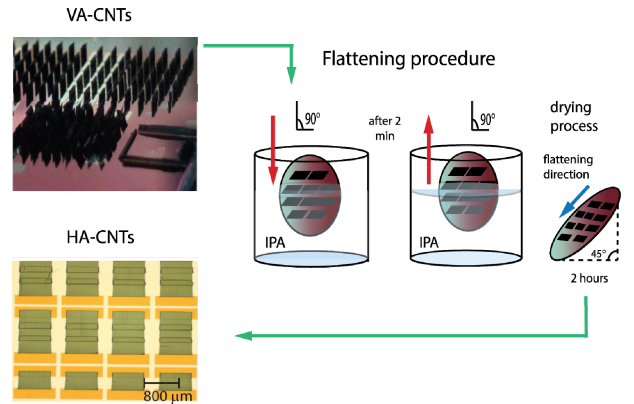


Figure 2: After the CVD growth the pre-patterned wafer with VA-CNTs (optical image) is immersed in IPA for 2 min and dried in ambient air under a fume hood. The resulting highly oriented HACNT sheets are shown in the optical image.

RESULTS AND DISCUSSION

The liquid-assisted flattening process shows good reproducibility and controllability thanks to the optimization of both the Fe catalyst shape and the wafer dipping phase. The variety of geometries and shapes obtained constitutes potential building blocks for MEMS devices (Fig. 3).

The SEM images in Fig. 4 show the morphological variation starting from the as-grown VA-CNT nanofoam, to densification process due to the IPA, ending with the coated HACNTs. The adopted deposition techniques allow nanoscale accuracy of the deposited layers. The average coating thickness obtained around the nanotube surface, 14.4 nm for the a-SiC and 12.5 nm for the Al₂O₃, is in agreement with the one measured on a bare Si wafer by ellipsometry (Woollam Ellipsometer).

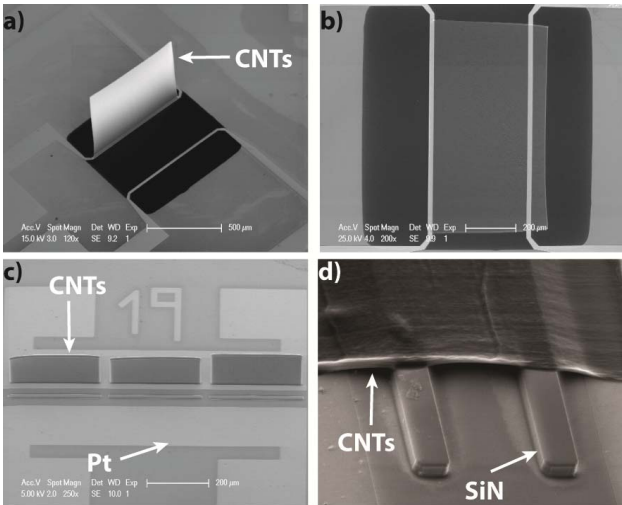


Figure 3: Examples of possible structures obtained by engineering the catalyst shape and by optimizing the flattening process. The SEM pictures show: (a) VA-CNTs grown on suspended Platinum (Pt) contacts before the flattening procedure; (b) After the IPA treatment a large area CNT membrane suitable for CNT-based gas sensors or actuators is obtained; (c) VA-CNTs grown on Pt to connect the contacts pads; (d) Suspended interconnects or thin-film self-sealing obtained after the flattening method.

As determined by SEM inspection, the regular foam-like VA-CNTs are packed with an estimated density of $77 \text{ tubes } \mu\text{m}^{-2}$. After the flattening procedure, the resulting HA-CNT morphology consists of compacted CNTs in which the initial alignment is retained. By starting from a rectangular VA-CNT with $W = 50 \mu\text{m}$, $T = 10 \mu\text{m}$ and $455 \mu\text{m}$ in height (H), the resulting HA-CNT substantially retains both the width (w) and the height (h) after the permutation, while the thickness, t , is the parameter that reflects the enhanced packing density. The densification ratio, defined as the ratio between the initial and the final thickness, $D_r = T/t$, is approximately 20. A subsequent increase in packing density of $\sim 1540 \text{ tubes } \mu\text{m}^{-2}$ is obtained.

Raman spectroscopy, performed at different stages of the process, shows the structural evolution from the uncoated vertically aligned CNTs to the hybrid composite creation (Fig. 5). The intensity ratio between the D-band ($\sim 1345 \text{ cm}^{-1}$) and the G-bands ($\sim 1586 \text{ cm}^{-1}$), I_D/I_G , indicates the quality variations. Specifically, the I_D/I_G

ratios are 0.67, 0.92, 1, and 0.97 for the VA-CNT, the HA-CNT, the $\text{Al}_2\text{O}_3/\text{HA}$ -CNT and the a-SiC/HA-CNT, respectively. The initial defectivity of the CNT is beneficial for the coating. In fact, the surface defects provide bonding sites for the coating nucleation. Therefore, no functionalization treatments are required on the CNT scaffold prior to the coating procedures.

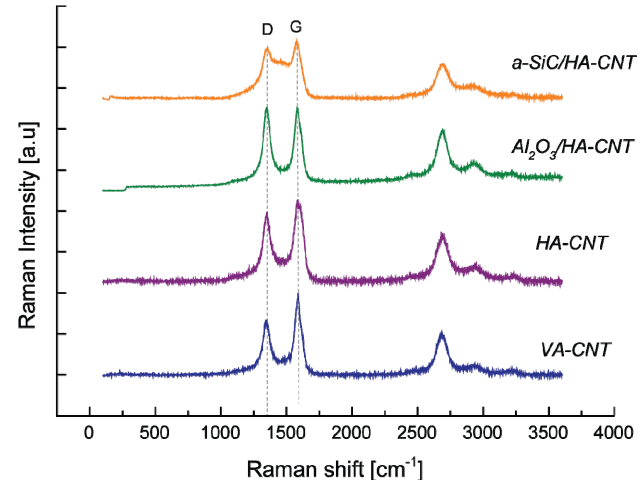


Figure 5: Raman spectra collected during the different stages of the fabrication process. The flattening process affects the as-grown CNT quality and a clearly hybrid composite is formed after the a-SiC coating.

The I-V characteristics of the a-SiC/HA-CNTs and the $\text{Al}_2\text{O}_3/\text{HA}$ -CNTs suspended membranes were measured and compared to the same samples before the coating procedure (Fig. 6). The measurements have been performed on HA-CNT sheets with $w = 800 \mu\text{m}$, $t = 6 \mu\text{m}$ and a distance between the electrodes of $400 \mu\text{m}$ (see inset Fig. 6).

The uncoated HA-CNT sheets exhibit a conductivity of $0.61 \text{ S}\cdot\text{cm}^{-1}$, while a substantial increase is recorded for the hybrid ones: 1.9 and $14.6 \text{ S}\cdot\text{cm}^{-1}$ for $\text{Al}_2\text{O}_3/\text{HA}$ -CNTs and a-SiC/HA-CNTs, respectively. The electrical conductivity enhancement induced by the conformal coatings demonstrates that the deposited thin layers help to overcome the high resistivity sites, corresponding to the junctions between neighbouring CNTs and defects along the nanotube. Moreover, it might likely be that the coating improves the anisotropic electrical transport of the CNT

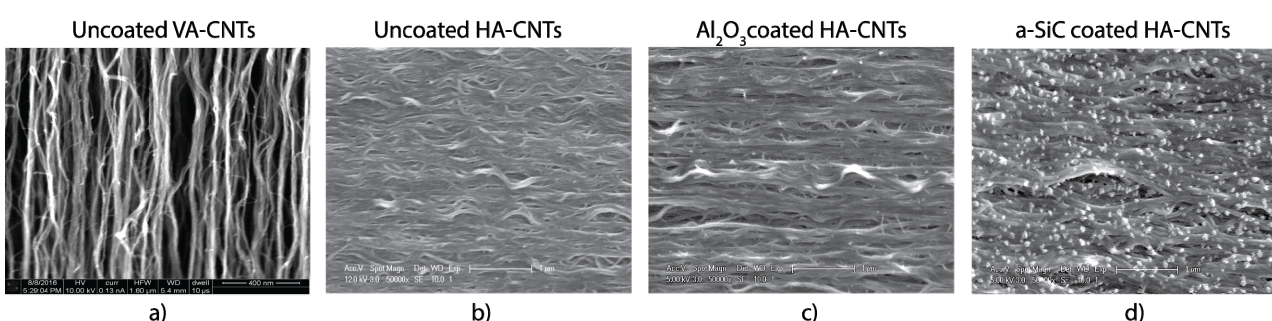


Figure 4: SEM close ups of the CNT morphology: (a) uncoated VA-CNT, (b) densified HA-CNT sheet, (c) Al_2O_3 hybrid sheet, (d) a-SiC hybrid sheet. The nanotube average diameter varies from 15 nm when uncoated to $39\text{-}44 \text{ nm}$ when coated.

and in particular, the one perpendicular to the tube axis.

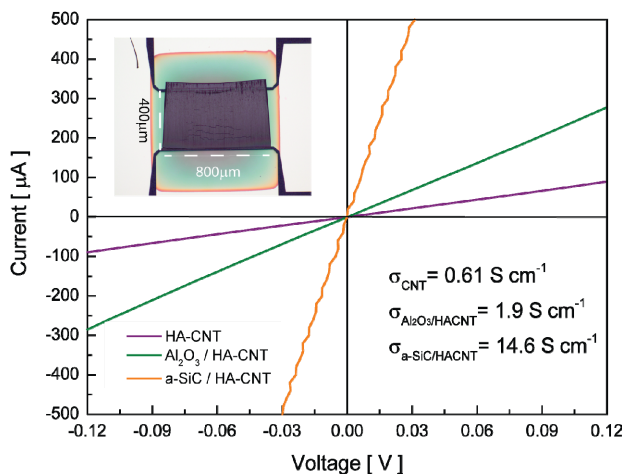


Figure 6: I-V curve before and after the coating procedure of the HA-CNT sheets (inset). The HA-CNT conductivity increases of ~209% by coating the sheets with Al_2O_3 and of ~2276% by adding a-SiC thin layer.

CONCLUSION

By combining the fast growth of long vertically aligned CNTs with a liquid-assisted flattening technique performed at wafer-scale, dense arrays of HA-CNTs with a densification ratio of approximately 20 are obtained. The resulting CNT network morphology is effectively used as scaffold to realize membranes and suspended interconnects. In fact, by coating the HA-CNTs with a targeted 10 nm layer of Al_2O_3 or a-SiC, an unprecedented enhancement in electrical conductivity is obtained: ~209% $\text{Al}_2\text{O}_3/\text{HA-CNTs}$ and 2276% for the a-SiC/HA-CNTs. The observed improvement due to the coating demonstrates the possibility to fine tune the response of CNT-based hybrid materials. This work clearly shows the CNT-based scaffold potential for functional building blocks to realize suspended interconnects, heat spreaders and novel chemical and optical sensors.

ACKNOWLEDGEMENTS

This work was supported by NanoNextNL, a micro and nano-technology consortium of the Government of the Netherlands and 130 partners. The authors gratefully acknowledge the technical staff of Else Kooi Laboratory at TU Delft for the support in device fabrication.

REFERENCES

- [1] X. Sun, T. Chen, Z. Yang, and H. Peng, “The Alignment of Carbon Nanotubes: An Effective Route To Extend Their Excellent Properties to Macroscopic Scale,” *Acc. Chem. Res.*, vol. 46, no. 2, pp. 539–549, Feb. 2013.
- [2] S. Vollebregt, F. D. Tichelaar, H. Schellevis, C. I. M. Beenakker, and R. Ishihara, “Carbon nanotube vertical interconnects fabricated at temperatures as low as 350°C,” *Carbon N. Y.*, vol. 71, pp. 249–256, 2014.
- [3] C. Silvestri, M. Riccio, R. H. Poelma, B. Morana, S. Vollebregt, F. Santagata, A. Irace, G. Q. Zhang, and P. M. Sarro, “Thermal characterization of carbon nanotube foam using MEMS microhotplates and thermographic analysis,” *Nanoscale*, vol. 8, no. 15, pp. 8266–75, 2016.
- [4] N. Gaio, C. Silvestri, B. van Meer, S. Vollebregt, C. Mummary, and R. Dekker, “Fabrication and characterization of an Upside-down Carbon Nanotube (CNT) Microelectrode array (MEA),” *IEEE Sens. J.*, pp. 1–1, 2016.
- [5] G. Fiorentino, S. Vollebregt, F. D. Tichelaar, R. Ishihara, and P. M. Sarro, “Impact of the atomic layer deposition precursors diffusion on solid-state carbon nanotube based supercapacitors performances,” *Nanotechnology*, vol. 26, no. 6, p. 64002, 2015.
- [6] J. Lu, J. Miao, T. Xu, B. Yan, T. Yu, and Z. Shen, “Growth of horizontally aligned dense carbon nanotubes from trench sidewalls,” *Nanotechnology*, vol. 22, no. 26, p. 265614, Jul. 2011.
- [7] H. Guerin, D. Tsamados, H. Le Poche, J. Dijon, and A. M. Ionescu, “In-situ grown horizontal carbon nanotube membrane,” *Microelectron. Eng.*, vol. 97, pp. 166–168, 2012.
- [8] S. Tawfick, K. O’Brien, and a. J. Hart, “Flexible high-conductivity carbon-nanotube interconnects made by rolling and printing,” *Small*, vol. 5, no. 21, pp. 2467–2473, Nov. 2009.
- [9] Y. Hayamizu, T. Yamada, K. Mizuno, R. C. Davis, D. N. Futaba, M. Yumura, and K. Hata, “Integrated three-dimensional microelectromechanical devices from processable carbon nanotube wafers.,” *Nat. Nanotechnol.*, vol. 3, no. 5, pp. 289–294, 2008.
- [10] M. De Volder, S. H. Tawfick, S. J. Park, D. Copic, Z. Zhao, W. Lu, and A. J. Hart, “Diverse 3D Microarchitectures Made by Capillary Forming of Carbon Nanotubes,” *Adv. Mater.*, vol. 22, no. 39, pp. 4384–4389, Oct. 2010.
- [11] T. Yamada, N. Makiomoto, A. Sekiguchi, Y. Yamamoto, K. Kobashi, Y. Hayamizu, Y. Yomogida, H. Tanaka, H. Shima, H. Akinaga, D. N. Futaba, and K. Hata, “Hierarchical three-dimensional layer-by-layer assembly of carbon nanotube wafers for integrated nanoelectronic devices,” *Nano Lett.*, vol. 12, no. 9, pp. 4540–4545, 2012.
- [12] R. H. Poelma, B. Morana, S. Vollebregt, E. Schlangen, H. W. van Zeijl, X. Fan, and G. Q. Zhang, “Tailoring the Mechanical Properties of High-Aspect-Ratio Carbon Nanotube Arrays using Amorphous Silicon Carbide Coatings,” *Adv. Funct. Mater.*, vol. 24, no. 36, pp. 5737–5744, 2014.

CONTACT

*C. Silvestri, tel: +31-15-2781891;
c.silvestri@tudelft.nl